The Peculiar Coordination of Barium: Ab Initio Study of the Molecular and Electronic Structures of the Group 2 Dihydride Dimers M_2H_4 (M = Mg, Ca, Sr, Ba)

Martin Kaupp*,† and Paul von Ragué Schleyer‡

Contribution from Max-Planck-Institut für Festkörperforschung, Heisenbergstrasse 1, 7000 Stuttgart 80, Germany, and Institut für Organische Chemie, Universität Erlangen-Nürnberg, Henkestrasse 42, 8520 Erlangen, Germany

Received June 10, 1993®

Abstract: Ab initio pseudopotential calculations at the SCF and MP2 levels of theory on the dimeric alkaline-earth dihydrides M_2H_4 (M = Mg, Ca, Sr, Ba) reveal interesting trends down group 2. In particular, barium prefers coordination environments which contradict simple ionic or VSEPR model expectations. The lowest-energy structure for Ba_2H_4, and for Sr_2H_4, is a triply hydride-bridged C_{3v} arrangement **4** with only one terminal hydrogen instead of the doubly bridged planar D_{2h} structure **1**. The latter would be expected for electrostatic reasons and is most stable for the lighter congeners (Be_2H_4, Mg_2H_4, Ca_2H_4). However, for Ba_2H_4 and Sr_2H_4, the D_{2h} structure **1** is not even a minimum on the HF potential energy surface but distorts to a C_{2h} structure **2** with pyramidal metal coordination. Even a quadruply bridged D_{4h} structure with extremely anisotropic metal coordination becomes competitive for Ba_2H_4. Harmonic vibrational frequencies for the minima on the M_2H_4 potential energy surfaces are given to facilitate the experimental discrimination among different structural possibilities. The present results are directly related to the unsymmetrical metal coordination in the solid-state structures of several barium amides and alkoxides. The unusual structural preferences of the heavier group 2 metals Sr and particularly Ba are also related to the bent structures of various MX_2 compounds of Sr, Ba, Eu, and Sm. The electronic reasons for this tendency toward low-symmetrical metal coordination include d-orbital involvement in bonding, cation polarization, and low interanionic repulsion. The same effects may be important for larger clusters or even for extended structures of group 2 or lanthanide(II) compounds.

I. Introduction

The calcium, strontium, and barium dihydrides are the simplest MX_2 compounds of these elements. Thus, their structural and electronic properties may serve as general models for an understanding of the principles of heavy alkaline-earth metal coordination chemistry. While the solid-state structures of CaH_2, SrH_2, and BaH_2 are known[1] (a $PbCl_2$-type structure in all three cases, in contrast to MgH_2, which prefers the simpler rutile structure[2]), no experimental data are yet available for the heavy alkaline-earth dihydrides in the gas phase.

We have recently studied the monomeric dihydrides by ab initio calculations.[3] The basic question, do these triatomic molecules prefer linear or bent structures, could be answered as follows: CaH_2 is linear but extremely "floppy", SrH_2 is bent but also has a very small bending force constant, and BaH_2 is genuinely bent (with a linearization energy of ca. 6 kcal/mol). The bent structures are fascinating, as they contradict the expectations of all simple models for main-group structural chemistry, e.g. the VSEPR model.[4] These[3] and other[5-12] computational results have widened and partially resolved the long-standing discussion[10] on the gas-phase equilibrium structures of the heavy alkaline-earth dihalides.

What are the preferred structures for coordination numbers larger than two? Ab initio calculations on $M^{+2}(L)_3$ (M = Sr, Ba; L = H_2O, NH_3) predict pyramidal metal coordination.[7] Recent X-ray crystal structures of the dimeric amides $(M[N(SiMe_3)_2]_2)_2$ (M = Mg, Ca, Sr, Ba)[14] indicate an exactly trigonal planar environment for magnesium as in **1** (dictated by space-group

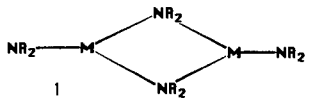

1

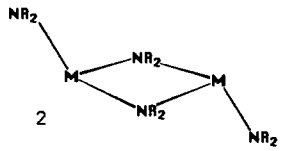

2

symmetry),[14a] a slight pyramidalization for the calcium and strontium complexes,[14b,c] and a significantly pyramidal coordi-

† Max-Planck-Institut für Festkörperforschung.

‡ Universität Erlangen-Nürnberg.

® Abstract published in *Advance ACS Abstracts*, October 15, 1993.

(1) Andresen, A. F.; Maeland, A. J.; Slotfeldt-Ellingsen, D. *J. Solid State Chem.* **1977**, *20*, 93. Bergsma, J.; Loopstra, B. O. *Acta Crystallogr.* **1962**, *15*, 92. Zintl, E.; Harder, A. *Z. Elektrochem.* **1935**, *41*, 33. Bronger, W.; Ci-Chien, S.; Müller, P. *Z. Anorg. Allg. Chem.* **1987**, *545*, 69.

(2) Zachariasen, W. H.; Holley, C. E., Jr.; Stamper, J. F., Jr. *Acta Crystallogr.* **1963**, *16*, 352.

(3) Kaupp, M.; Schleyer, P. v. R.; Stoll, H.; Preuss, H. *J. Chem. Phys.* **1991**, *94*, 1360.

(4) See, e.g.: Gillespie, R. J.; Hargittai, I. *The VSEPR Model of Molecular Geometry*; Allyn and Bacon: Boston, MA, 1991.

(5) Kaupp, M.; Schleyer, P. v. R. *J. Am. Chem. Soc.* **1992**, *114*, 491.

(6) Kaupp, M.; Schleyer, P. v. R.; Dolg, M.; Stoll, H. *J. Am. Chem. Soc.* **1992**, *114*, 8202. Kaupp, M.; Charkin, O. P.; Schleyer, P. v. R. *Organometallics* **1992**, *11*, 2767.

(7) (a) Kaupp, M.; Schleyer, P. v. R. *J. Phys. Chem.* **1992**, *96*, 7316. (b) Bauschlicher, C. W., Jr.; Sodupe, M.; Partridge, H. *J. Chem. Phys.* **1992**, *96*, 4453.

(8) Jolly, C. A.; Marynick, D. S. *Inorg. Chem.* **1989**, *28*, 2893.

(9) Dolg, M.; Stoll, H.; Preuss, H. *THEOCHEM* **1991**, *235*, 67.

(10) The first experimental evidence for bent alkaline-earth metal dihalide structures came from early electric quadrupole deflection experiments of Klemperer et al.: Büchler, A.; Stauffer, J. L.; Klemperer, W.; Wharton, L. *J. Chem. Phys.* **1963**, *39*, 2299. Bent alkaline earth metallocene structures are discussed in Hanusa, T. P. *Polyhedron* **1990**, *9*, 1345 and various references cited therein. For the most recent reviews, cf. refs 11–13 and also refs 3 and 5–7. Also see: Kaupp, M.; Schleyer, P. v. R.; Stoll, H. *J. Phys. Chem.* **1992**, *96*, 9801–9805.

(11) Seijo, L.; Barandiaran, Z.; Huzinaga, S. *J. Chem. Phys.* **1991**, *94*, 3762.

(12) Kaupp, M.; Schleyer, P. v. R.; Stoll, H.; Preuss, H. *J. Am. Chem. Soc.* **1991**, *113*, 6012.

(13) Hargittai, M. *Coord. Chem. Rev.* **1988**, *91*, 35.

(14) (a) Westerhausen, M.; Schwarz, W. *Z. Anorg. Allg. Chem.* **1992**, *609*, 39. (b) Westerhausen, M.; Schwarz, W. *Z. Anorg. Allg. Chem.* **1991**, *604*, 127. The average Ca–Ca–N_t angle is ca. 169°. (c) Westerhausen, M.; Schwarz, W. *Z. Anorg. Allg. Chem.* **1991**, *606*, 177. The average Sr–Sr–N_t angle is ca. 169°. (d) Vaartstra, B. A.; Huffman, J. C.; Streib, W. E.; Caulton, K. G. *Inorg. Chem.* **1991**, *30*, 121. The Ba–Ba–N_t angle is 158.3°.

0002-7863/93/1515-11202$04.00/0

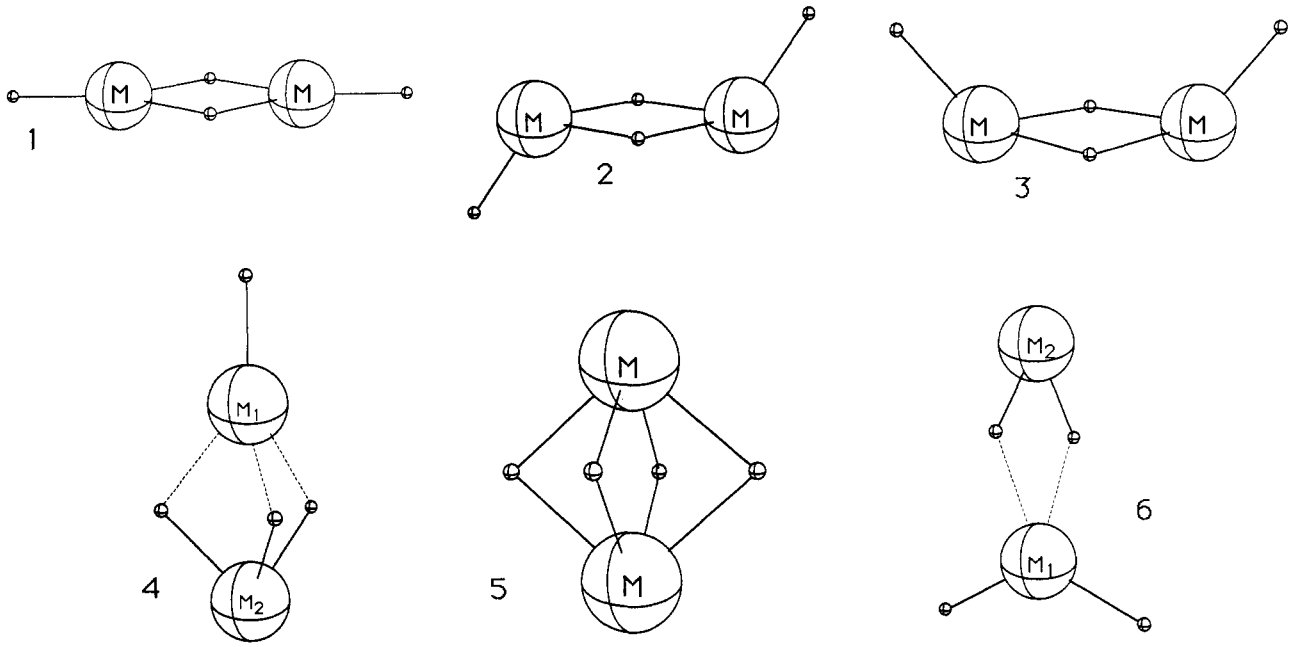

Figure 1. Schematic representations of possible M_2H_4 structures: (top left) planar D_{2h} **1**, (top middle) C_{2h} **2** with pyramidal metal coordination and *trans* arrangement of the terminal ligands, (top right) C_{2v} **3** with pyramidal metal coordination and *cis* arrangement of the terminal ligands, (bottom left) triply bridged C_{3v} **4**, (bottom middle) quadruply bridged D_{4h} **5**, (bottom right) C_{2v} **6** with both terminal ligands bound to a single metal atom.

nation for barium[14d] as in **2**. The X-ray structural analysis of the barium complex $BaCb_2(DME)_3$ (Cb = carbazolyl, DME = dimethoxyethylene) and ab initio model calculations on $Ba(NH_2)_2(HF)_4$ have revealed a cisoid preference of the anionic ligands (carbazolyl and NH_2, respectively) in spite of the increased anion–anion repulsions (in contrast to the corresponding calcium species).[15]

Thus, the extensively studied electronic influences that lead to bent monomeric MX_2 structures[5-7,11,12] may also influence the structures of higher-coordinate species. To obtain further insight into the rules that determine the molecular structures of heavy group 2 compounds with metal coordination numbers larger than two, we have now extended our theoretical study of the monomeric Ca, Sr, and Ba dihydrides[3] to the dimers M_2H_4. For comparison, Mg_2H_4 also has been computed. These model species are still simple enough to be studied by accurate ab initio methods, and it has been possible to investigate a number of alternative possible geometries. The structures we propose for the BaH_2 and SrH_2 dimers differ dramatically from expectations based on simple ionic arguments or on VSEPR model[4] rules. We hope that the calculated vibrational frequencies given will stimulate the experimental study of these fascinating gas-phase species. After completion of the present work, Drake et al. reported the solid-state structures of some dinuclear barium alkoxides and siloxides with extremely unsymmetrical metal coordination.[16] These are directly related to the unusual structures predicted for Ba_2H_4 and Sr_2H_4 and will also be discussed in this context.

II. Computational Methods

Full gradient structure optimizations at the Hartree–Fock and MP2 levels of theory[17] have been carried out with the Gaussian 90[18] and Gaussian 92[19] programs. The calculations involved the same quasirelativistic 10-valence-electron pseudopotentials and 6s6p5d valence basis sets for Ba, Sr, and Ca,[3] as well as the 2-valence-electron pseudopotential with (4s2p)/[3s2p] valence basis for Mg,[20] used in our previous theoretical studies of alkaline-earth metal compounds[3,5-7a,12,15] (the frozen-core 2-valence-electron pseudopotential approach for Mg has been found to excellently reproduce all-electron calculations for a variety of species[12,20b]). A (4s1p)/[2s1p] basis[21] was employed on hydrogen. For preliminary optimizations and for the harmonic vibrational frequency analyses, the basis sets for the heavier metals have been contracted to 21111/21111/311.[22] The basis set contraction does not alter the structures appreciably (however, note the differences for the C_{2h} structure of Sr_2H_4, section III), and so only the SCF and MP2 bond lengths and angles obtained with the uncontracted basis sets will be given. The MP2 calculations correlated all electrons available outside the pseudopotential cores.

III. Comparison of the Relative Stabilities of Different Stationary Points

The structures considered are shown schematically in Figure 1. The planar D_{2h} structure **1** (Figure 1, top left), the C_{2h} structure **2** (Figure 1, top middle), the C_{3v} structure **4** (Figure 1, bottom left), and the D_{4h} structure **5** (Figure 1, bottom middle) have been computed at the MP2 and HF levels for all four metals. The C_{2v} alternative **6** (Figure 1, bottom right) has been calculated at

(15) Mösges, G.; Hampel, F.; Kaupp, M.; Schleyer, P. v. R. *J. Am. Chem. Soc.* **1992**, *114*, 10880–10889.
(16) Drake, S. R.; Streib, W. E.; Folting, K.; Chisholm, M. H.; Caulton, K. G. *Inorg. Chem.* **1992**, *31*, 3205.
(17) For explanations of standard levels of ab initio MO theory, see e.g.: Hehre, W. J.; Radom, L.; Schleyer, P. v. R.; Pople, J. A. *Ab Initio Molecular Orbital Theory*; Wiley: New York, 1986.
(18) Frisch, M. J.; Head-Gordon, M.; Trucks, G. W.; Foresman, J. B.; Schlegel, H. B.; Raghavachari, K.; Robb, M.; Binkley, J. S.; Gonzalez, C.; DeFrees, D. J.; Fox, D. J.; Whiteside, R. A.; Seeger, R.; Melius, C. F.; Baker, J.; Kahn, L. R.; Stewart, J. J. P.; Topiol, S.; Pople, J. A. *Gaussian 90*, Revision F; Gaussian, Inc.: Pittsburgh, PA, 1990.
(19) Frisch, M. J.; Trucks, G. W.; Head-Gordon, M.; Gill, P. M. W.; Wong, M. W.; Foresman, J. B.; Johnson, B. G.; Schlegel, H. B.; Robb, M. A.; Replogle, E. S.; Gomperts, R.; Andres, J. L.; Raghavachari, K.; Binkley, J. S.; Gonzalez, C.; Martin, R. L.; Fox, D. I.; DeFrees, D. J.; Baker, J.; Stewart, J. P.; Pople, J. A. *Gaussian 92*, Revision A; Gaussian, Inc.: Pittsburgh, PA, 1992.
(20) (a) Fuentealba, P.; v. Szentpály, L.; Preuss, H.; Stoll, H. *J. Phys. B* **1985**, *73*, 1287. (b) Kaupp, M.; Stoll, H.; Preuss, H. *J. Comput. Chem.* **1990**, *11*, 1029. (c) Fuentealba, P.; Reyes, O.; Stoll, H.; Preuss, H. *J. Chem. Phys.* **1987**, *87*, 5338.
(21) Dunning, T. H.; Hay, P. J. In *Methods of Electronic Structure Theory*; Modern Theoretical Chemistry, Vol. 3; Schaefer, H. F., III, Ed.; Plenum Press: New York, 1977.
(22) The first and third contraction coefficients for the first s shell of the barium valence basis set given in ref 3 are in error: they should read –5.928 895 and –0.551 437 instead of –5.328 895 and –0.351 437, respectively.

Table I. Relative Stabilities of Different Stationary Points on the Potential Energy Surfaces of M_2H_4 (M = Mg, Ca, Sr, Ba) and Dimerization Energies (kcal/mol)

	Mg_2H_4			Ca_2H_4		
structure	HF	NIMAG[a]	MP2	HF	NIMAG[a]	MP2
D_{2h}	0.0	0	0.0	0.0	0	0.0
C_{3v}	+28.4	2	+27.5	+4.1	0	+1.4
D_{4h}	+122.7	3	+121.3	+38.1	0	+31.2
C_{2v} (6)[b]	→2 × MgH_2		→2 × MgH_2	34.5	1	
2 × MH_2	+25.1	0	+27.6	+48.0	0	+51.5

	Sr_2H_4			Ba_2H_4		
structure	HF	NIMAG[a]	MP2	HF	NIMAG[a]	MP2
C_{2h}	+2.0	0	+4.6	+5.3	0	+8.5
D_{2h}	+2.0	2[c]	+4.8	+9.8	2	+13.4
C_{3v}	0.0	0	0.0	0.0	0	0.0
D_{4h}	+24.6	0	+20.7	+12.6	0	+8.0
C_{2v} (6)[b]	+31.0	1		+30.6	1	
C_{2v} (3)[d]				+7.1	0	
2 × MH_2	+52.3	0	+57.9	+53.9	0	+60.3

[a] Number of imaginary frequencies in the HF vibrational frequency analysis. [b] Structure with two terminal hydrogens bound to the same metal, cf. Figure 1, bottom right. [c] This structure is a minimum at the standard basis-set level used for the frequency calculations but exhibits two imaginary frequencies with the uncontracted metal basis set. [d] Cf. Figure 1, top right.

Table II. Zero-Point Vibrational Energies (kcal/mol) for Various M_2H_4 Stationary Points[a]

M	D_{2h} (1)	C_{2h} (2)	C_{2v} (3)	C_{3v} (4)	D_{4h} (5)	2 × MH_2
Mg	15.1			14.1	12.7	12.4
Ca	11.6			12.8	12.7	8.6
Sr	10.2	10.2		11.7	12.3	7.4
Ba	9.2	9.8	9.6	10.8	12.2	7.2

[a] Hartree–Fock results.

HF for M = Ca, Sr, and Ba (for M = Mg, it dissociates into two monomers, both at the HF and MP2 levels of theory, cf. below). The C_{2v} structure **3** (Figure 1, top right) has only been studied for M = Ba. Optimization of Ba_2H_4 in C_s symmetry with a single hydrogen bridge, as considered for Be_2H_4 by DeFrees et al.,[23] converged to structure **6**.

The relative energies of various structural possibilities and the nature of these stationary points (number of imaginary frequencies, NIMAG) on the M_2H_4 potential energy surfaces (PES) are shown in Table I. Table II gives the zero-point vibrational energies. The structural features will be discussed in section IV. Obviously, with the exception of the C_{3v} and D_{4h} forms of Mg_2H_4, all structures calculated are bound with respect to the separated monomers. The high ionicity of the M–H bonds for the heavier metals (cf. section V) leads to a large electrostatic stabilization of all arrangements with alternating metal dications and hydride anions, to which our study has been restricted. Note the much larger dimerization energies for the Ca, Sr, and Ba dihydrides compared to MgH_2.

Both Mg_2H_4 and Ca_2H_4 apparently favor the doubly bridged planar D_{2h} structure **1**. This nuclear configuration would be expected to afford the best arrangement of point charges, as it minimizes anion–anion repulsions but maximizes the anion–cation attractions. The same structure has already also been found computationally for Be_2H_4[23-26] and for Mg_2H_4;[26] optimizations of both in C_{2h} symmetry (stucture **2**) converge to the planar D_{2h} arrangements. For Mg_2H_4 the triply bridged C_{3v} structure **4** lies ca. 28 kcal/mol higher in energy and exhibits two imaginary frequencies at the HF level. Moreover, it is unbound with respect to the separated dihydride monomers (in agreement with the calculations of Kirillov et al.[26]). However, for Ca_2H_4, C_{3v} structure **4** is an HF minimum, only ca. 1–2 kcal/mol higher in energy (at the MP2 level) than the D_{2h} arrangement.

In contrast to Mg_2H_4 and Ca_2H_4, the D_{2h} Ba_2H_4 structure is not an HF minimum (Table I), and the C_{2h} structure **2** with pyramidal metal coordination is significantly more stable (ca. 5 kcal/mol). The C_{2h}–D_{2h} energy difference is negligible for strontium, and contraction of the metal basis set, as used for the frequency calculations, leads to a D_{2h} minimum (a similar basis-set dependence was noted for the bending angle in quasilinear MX_2 species like CaF_2, $SrCl_2$, or BaI_2[11,12]). This behavior correlates with the linearization energies found for the monomeric dihydrides, ca. 6 kcal/mol for BaH_2, but only ca. 1 kcal/mol for SrH_2[3] (MgH_2 is linear,[27] CaH_2 is linear but with a shallow bending potential[3]). Thus, the increasing pyramidalization of the metal coordination in the dimeric diamides $\{M[N(SiMe_3)_2]_2\}_2$ (cf. the Introduction)[14] in going from M = Mg to M = Ba is reflected in the relative energies of the C_{2h} **2** vs the D_{2h} **1** structures of the dihydride dimers.

However, the triply bridged C_{3v} form **4** (a minimum on the PES for Ca_2H_4, Sr_2H_4, and Ba_2H_4) is even lower in energy than the C_{2h} arrangement **2** both for Sr_2H_4 and Ba_2H_4. The C_{3v} vs C_{2h} preference is increased by electron correlation (by ca. 2–4 kcal/mol) and is as large as ca. 8.5 and 4.5 kcal/mol at MP2 for the barium and strontium species, respectively. Consistent with the size and polarizability of the cation, as well as d-orbital participation of (cf. section V), the preference for this extremely unsymmetrical metal coordination is largest for barium.

The quadruply bridged D_{4h} arrangement **5** (Figure 1, bottom middle) is also a minimum on the HF PES for Ca_2H_4, Sr_2H_4, and Ba_2H_4 but is higher in energy than the C_{3v} structures (for Mg_2H_4, **5** has three imaginary frequencies and lies ca. 120 kcal/mol higher than **1** and ca. 90 kcal/mol higher than the separated monomers, consistent with the results of Kirillov et al.[26]). However, while the energy difference for D_{4h} vs D_{2h} or C_{2h} structures is ca. 30 kcal/mol for M = Ca and ca. 20 kcal/mol for M = Sr, the D_{4h} structure for Ba_2H_4 becomes competitive to the C_{2h} form (Table I). Thus, both C_{3v} and D_{4h} arrangement become more favorable in going from Mg to Ba. We note that the contributions from electron correlation for Ca_2H_4, Sr_2H_4, and Ba_2H_4 follow the order $D_{4h} > C_{3v} > C_{2h} > D_{2h}$, i.e. they decrease with increasingly symmetrical metal coordination of (cf. MP2 vs HF results in Table I).

The C_{2v} structure **3** (Figure 1c) has only been calculated for $(BaH_2)_2$. The HF results (Table I) indicate that this cis arrangement also is a minimum but is slightly less favorable than the trans C_{2h} alternative **2**. Interestingly, the ca. 2 kcal/mol C_{2v} vs C_{2h} energy difference is similar to the corresponding differences computed for M_2H_4 (M = Ge, Sn, Pb) by Trinquier.[28a]

Structures **6** with two terminal hydrogen atoms bound to the same metal have been considered at the HF level for M = Ca, Sr, and Ba. While the energies are considerably higher than for the other structures, these forms are still bound with respect to two MH_2 monomers. All exhibit one imaginary frequency (in a B_2 mode), which corresponds to a transformation into the C_{3v} structures **4**. As indicated above, optimization of **6** for Mg_2H_4 leads to the dissociated monomers. Note that in this case even **4** exhibits two imaginary frequencies and no significant stabilization vs the monomers. These results are consistent with a relatively low polarity of the Mg–H bonds compared to those of the heavier metals (cf. above).

(23) DeFrees, D. J.; Raghavachari, K.; Schlegel, H. B.; Pople, J. A.; Schleyer, P. v. R. *J. Phys. Chem.* **1987**, *91*, 1857.
(24) Ahlrichs, R. *Theor. Chim. Acta* **1970**, *17*, 348.
(25) (a) Cimiraglia, R.; Persico, M.; Tomasi, J.; Charkin, O. P. *J. Comput. Chem.* **1984**, *5*, 263. (b) Sukhanov, L. P.; Boldyrev, A. I.; Charkin, O. P. *Chem. Phys. Lett.* **1983**, *97*, 373. (c) Sukhanov, L. P.; Boldyrev, A. I.; Charkin, O. P. *Koord. Khim.* **1983**, *9*, 762.
(26) Kirillov, Y. B.; Boldyrev, A. I.; Klimenko, N. M.; Charkin, O. P. *J. Struct. Chem.* **1983**, *24*, 134.
(27) Chaquin, P.; Sevin, A.; Yu, H. *J. Phys. Chem.* **1985**, *89*, 2813.
(28) (a) Trinquier, G. *J. Am. Chem. Soc.* **1990**, *112*, 2130. (b) Trinquier, G.; Barthelat, J.-C. *J. Am. Chem. Soc.* **1990**, *112*, 9121.

Table III. HF (MP2) Bond Distances (Å) and Angles (deg) for the D_{2h} and C_{2h} M_2H_4 Structures **1** and **2**[a]

D_{2h} (**1**)

M	Mg	Ca	Sr	Ba
M–H_t	1.693 (1.688)	2.069 (2.038)	2.245 (2.215)	2.428 (2.404)
M–H_b	1.877 (1.870)	2.226 (2.198)	2.417 (2.378)	2.629 (2.585)
M–M	2.830 (2.822)	3.526 (3.456)	3.846 (3.786)	4.214 (4.142)
M–H_b–M	97.9 (98.0)	103.7 (103.6)	105.4 (105.5)	106.5 (106.5)

C_{2h} (**2**)

M	Mg[b]	Ca[b]	Sr	Ba
M–H_t			2.238 (2.208)	2.386 (2.353)
M–H_b			2.414 (2.372)	2.568 (2.522)
M–M			3.846 (3.780)	4.182 (4.112)
M–H_b–M			105.6 (105.6)	109.0 (109.2)
H_t–M–M			159.1 (159.2)	123.4 (125.7)

[a] Hartree–Fock results with MP2 values in parentheses. Notation: H_b = bridging hydrogen, H_t = terminal hydrogen, cf. Figure 1, top left and top middle. [b] Cf. D_{2h}.

Table IV. HF (MP2) Bond Distances (Å) and Angles (deg) for the C_{3v} M_2H_4 Structures **4**[a]

M	Ca	Sr	Ba
M(1)–H_t	2.083 (2.052)	2.261 (2.231)	2.452 (2.429)
M(1)–H_b	2.376 (2.315)	2.539 (2.478)	2.719 (2.655)
M(2)–H_b	2.129 (2.089)	2.286 (2.243)	2.457 (2.412)
M(1)–M(2)	3.086 (3.024)	3.590 (3.528)	3.740 (3.678)
M(1)–H_b–M(2)	93.7 (93.4)	90.9 (90.5)	87.6 (87.0)

[a] Cf. Figure 1, bottom left.

Table V. HF (MP2) Bond Distances (Å) and Angles (deg) for the D_{4h} M_2H_4 Structures **5**[a]

M	Ca	Sr	Ba
M–H	2.251 (2.198)	2.399 (2.345)	2.550 (2.497)
M–M	2.736 (2.678)	3.024 (2.966)	3.346 (3.288)
M–H–M	74.9 (75.1)	78.2 (78.4)	82.0 (82.4)

[a] Cf. Figure 1, bottom center.

Table VI. HF Bond Distances (Å) and Angles (deg) for the Unsymmetrically Bridged C_{2v} M_2H_4 Structures **6** (M = Ca, Sr, Ba)[a]

	Ca	Sr	Br
M(1)–H_t	2.121	2.295	2.462
M(1)–H_b	2.561	2.700	2.898
M(2)–H_b	2.030	2.180	2.339
M(1)–M(2)	3.485	3.826	4.248
M(1)–H_b–M(2)	98.1	102.7	107.9
H_t–M(1)–H_t	148.8	140.7	128.4

[a] Cf. Figure 1, bottom right.

IV. Bond Distances and Bond Angles

Important bond distances and angles for the M_2H_4 structures are summarized in Tables III–VI. In general, the MP2 distances (given in parentheses) are slightly shorter than the HF values for the three heavier metals (Ca, Sr, Ba). This is due to core–valence correlation, a well-known effect in compounds of the heavy group 1 and 2 elements.[3,12,20c,29] Larger basis sets in the MP2 calculations would probably lead to a further contraction by ca. 0.02–0.08 Å.[3,12] Bond angles are affected only slightly by correlation. Data for Mg_2H_4 (note the frozen-core 2-valence-electron description employed) are less correlation dependent than those for the heavier metals (cf. Table III). This was found in previous pseudopotential and all-electron calculations on magnesium compounds (see, e.g., refs 12 and 20b,c).

***C*$_{2h}$ 2 vs *D*$_{2h}$ 1 Structures.** The basic difference between the C_{2h} and D_{2h} structures (Table III) is the out-of-plane orientation of the terminal hydrogen atoms, as measured by the H_t–M–M angle. This differs significantly from 180° for $(BaH_2)_2$, but less so for $(SrH_2)_2$ (compare ref 14). In going from planar (D_{2h}) to pyramidal (C_{2h}) metal environments in $(BaH_2)_2$, all bond lengths decrease by ca. 0.04 Å, similar to the (somewhat larger, ca. 0.10 Å) bond contraction observed between linear and bent BaH_2.[3] The M–H_b–M angles increase by ca. 2.5° from D_{2h} to C_{2h}. The bridging M–H distances are ca. 0.15–0.20 Å larger than the terminal M–H distances, which are similar to those in the monomers.[3] While the M–M distances are shorter than those in the bulk metals, they are considerably larger than the sums of the dication radii. Bonding analyses show only little direct metal–metal bonding. The bond lengths and angles in the C_{2v} structure **3** of Ba_2H_4 are close to those of the C_{2h} arrangement.

***C*$_{3v}$ Structures 4.** As the M(1)–H_b and M(2)–H_b distances in Table IV reveal, the M(1)–H–M(2) bridges are very unsymmetrical: the M(2)–H_b bond lengths to the tricoordinated metal atom are about the same as those of the terminal M(2)–H_t bonds, whereas the M(1)–H_b distances are considerably (ca. 0.25 Å) larger. Thus, the description as an ion pair complex $HM^+{\cdot}H_3M^-$ is appropriate. The coordination of both M(1) and M(2) is extremely unsymmetrical. The M(1)–H_t distances are only ca. 0.02 Å longer than those in the D_{2h} and C_{2h} structures **1** and **2** (cf. Table III).

The angles at the bridging hydrogen atoms are smaller (ca. 90°) than those found for structures **1** or **2** (ca. 105°). This leads to shorter M–M distances.

***D*$_{4h}$ Structures 5.** Due to the presence of four equivalent bridging hydrogen atoms, the metal atoms in structure **5** are very anisotropically coordinated (cf. Figure 1, bottom middle). The M–H bond lengths (cf. Table V) are closest to the bridging M–H_b distances in the D_{2h} or C_{2h} structures. With M = Ca, the bridging distances in structures **1** and **5** are almost equal. This reflects the unfavorable bonding in the D_{4h} structure **5**, compared to **1**, due to the smaller size of calcium (cf. energetic considerations in the preceding section).

The angles at the bridging hydrogen atoms are even smaller (ca. 75–80°) than for the C_{3v} structures **4**, and the M–M distances are quite short (but still considerably larger than the sums of the ionic radii).

***C*$_{2v}$ Structures 6.** The structural parameters obtained for structures **6** of $(MH_2)_2$ (M = Ca, Sr, Ba), with two terminal hydrogen atoms attached to the same metal, are summarized in Table VI. Structure **6** (cf. Figure 1, bottom right) may be characterized as a rather weakly bound (cf. section III) head-to-tail aggregate of two MH_2 units. The very long M(1)–H_b distances are the most prominent features. The M–M distances are larger than those in any of the other structures considered.

V. Electronic Origins of the Structural Preferences

Computational studies on a large number of monomeric MX_2 compounds (M = Ca, Sr, Ba)[3,5,6,11,12] and on some cationic complexes[7] have delineated the factors that control the bent or linear preferences. Polarization of the metal dication by the ligands and small but significant covalent σ-bonding contributions, involving metal d orbitals, lead to bending. Anion–anion repulsion, anion polarization,[12] and π-bonding contributions (between appropriate ligand orbitals and acceptor π orbitals on the metal[5,8]) favor linear arrangements. The balance between these factors determines the structures of heavy alkaline-earth MX_2 species (and, e.g., those of the corresponding lanthanide(II) compounds[6,9]). Due to the large size and polarizability of the barium dication, as well as the availability of vacant d orbitals, BaX_2 compounds exhibit the largest deviations from linearity. Even when additional neutral coligands L are present, i.e. in $BaX_2(L)_n$, the anionic ligands X may prefer cisoid over transoid arrangements.[15]

In view of these findings, and those for tricoordinated $M^{+n}(L)_3$ complexes,[7,8] the stability of the unusual C_{3v} structure **4** and the

(29) (a) Partridge, H.; Bauschlicher, C. W.; Walch, S. P.; Liu, B. *J. Chem. Phys.* **1983**, *72*, 1866. (b) Pettersson, L. G. M.; Siegbahn, P. E. M.; Ismail, S. *Chem. Phys.* **1983**, *82*, 355. (c) Jeung, G.; Daudey, J.-P.; Malrieu, J.-P. *Chem. Phys. Lett.* **1983**, *98*, 433.

Table VII. Metal NPA Charges (Q) and Valence Populations for the C_{2h} and D_{2h} $(BaH_2)_2$ Structures, as Well as for Linear and Bent BaH_2

	$(BaH_2)_2$[a]		BaH_2[b]	
	C_{2h}	D_{2h}	bent	linear
Q(M)	1.612	1.645	1.568	1.625
s	0.254	0.218	0.261	0.198
p_x	0.015	0.000	0.000	0.000
p_y	0.013	0.007	0.049	0.103
p_z	0.007	0.039	0.010	0.000
p_{tot}[c]	0.035	0.046	0.059	0.103
d_{xy}	0.042	0.000	0.000	0.000
d_{xz}	0.001	0.000	0.001	0.000
d_{yz}	0.032	0.030	0.077	0.000
$d_{x^2-y^2}$	0.019	0.005	0.049	0.058
d_{z^2}	0.018	0.059	0.003	0.020
d_{tot}[d]	0.112	0.094	0.130	0.078

[a] The $Ba_2H_{(b)2}$ ring plane is the yz plane (cf. Figure 1, top middle). [b] The molecule lies in the yz plane. [c] Sum of the p populations. [d] Sum of the d populations.

competitiveness of the D_{4h} structure **5** for Ba_2H_4 can be attributed to cation polarization and to d-orbital participation in covalent bonding. The relatively large anion–anion distances also result in smaller interanionic repulsions than for the Ca or Sr congeners. The same factors are responsible for the distortion of the doubly bridged D_{2h} structure **1** (the most stable form for Be_2H_4,[23-26] Mg_2H_4,[26] and Ca_2H_4) to a C_{2h} arrangement **2** for Ba_2H_4, which has pyramidal metal coordination (see below).

Cation polarization and d-orbital participation in bonding are interrelated.[3,30] The former may be visualized[30] by means of the electron localization function (ELF),[31] while the latter may be quantified[5-8,12] by natural population analysis (NPA).[32]

The NPA metal charges and valence populations for Ba_2H_4 with C_{2h} and D_{2h} structures, as well as for bent and linear BaH_2, are compared in Table VII. As has been shown for other BaX_2 compounds,[5,12] covalent bonding contributions are larger for the bent than for the linear BaH_2 structures (cf. metal charge Q(M)). The s and d_{yz} populations increase, due to more efficient sd hybridization in the bent arrangement. In contrast, the p_y populations are reduced somewhat.

A similar but smaller increase in the covalent bonding contributions (note smaller charge Q(M) in Table VII) is apparent when going from the D_{2h} to the C_{2h} structure of Ba_2H_4. Again, this is due to a greater degree of sd hybridization in the less symmetrical arrangement. Cation polarization also favors the less symmetrical structure, as has been shown for the dihydride and dihalide monomers[3,12] and for $Sr^{+2}(H_2O)_2$.[7b] The origin for the pyramidal coordination preference in Ba_2H_4 (C_{2h}) is indeed closely related to the bending in BaH_2.

Table VIII compares the NPA charges and metal populations for the $MH^+MH_3^-$ C_{3v} structures **4** of Ca_2H_4 and Ba_2H_4. While the M(1) atom belonging to the MH^+ fragment bears considerably less positive charge than M(2) for M = Ca, the M(1) and M(2) charges are more similar (in spite of the larger MH_3^- fragment charge, –0.822 vs –0.804) for M = Ba. This is due to the considerable s, d_{xz}, and d_{yz} populations for Ba(2). The strongly pyramidal BaH_3^- fragment is stabilized by sd hybridization (and by cation polarization). Ba(1) also is very anisotropically coordinated. These decisive factors favor the C_{3v} arrangement **4** which is the most stable form of Ba_2H_4 and Sr_2H_4. Moreover, the large charge separation for the $Ba(1)H^+$ fragment in **4** may lead to larger Coulombic and dipole–dipole interactions than for the calcium C_{3v} complex **4**.

(30) Kaupp, M. Ph.D. Dissertation, Universität Erlangen-Nürnberg, 1992.
(31) For descriptions of ELF, see: (a) Becke, A. D.; Edgecombe, K. E. *J. Chem. Phys.* **1990**, *92*, 5397. (b) Savin, A.; Becke, A. D.; Flad, J.; Nesper, R.; Preuss, H.; v. Schnering, H. G. *Angew. Chem.* **1991**, *103*, 421; *Angew. Chem., Int. Ed. Engl.* **1991**, *30*, 409.
(32) Reed, A. E.; Weinstock, R. B.; Weinhold, F. *J. Chem. Phys.* **1985**, *83*, 735.

Table VIII. NPA Charges (Q) and Metal Valence Populations for C_{3v} M_2H_4 **4** (M = Ca, Ba)[a]

	Ca		Ba	
M	M(1)	M(2)	M(1)	M(2)
Q(M)	1.547	1.619	1.625	1.635
$Q(H_t)$	–0.743		–0.803	
$Q(H_b)$		–0.807		–0.819
s	0.350	0.269	0.233	0.239
p_x	0.009	0.013	0.006	0.007
p_y	0.009	0.013	0.006	0.007
p_z	0.023	0.004	0.033	0.005
p_{tot}	0.041	0.030	0.045	0.018
d_{xy}	0.001	0.011	0.002	0.011
d_{xz}	0.014	0.034	0.020	0.052
d_{yz}	0.014	0.034	0.020	0.052
$d_{x^2-y^2}$	0.001	0.011	0.002	0.011
d_{z^2}	0.035	0.002	0.059	0.006
d_{tot}	0.065	0.092	0.103	0.132

[a] The C_3 axis lies in z direction. Cf. Figure 1, bottom left.

Table IX. NPA Metal Charges (Q) and Valence Populations for D_{4h} M_2H_4 **5** (M = Ca, Ba)[a]

M	Ca	Ba
Q(M)	1.630	1.630
s	0.226	0.209
p_x	0.016	0.008
p_y	0.016	0.008
p_z	0.002	0.003
p_{tot}	0.034	0.020
d_{xy}	0.000	0.000
d_{xz}	0.028	0.051
d_{yz}	0.028	0.051
$d_{x^2-y^2}$	0.062	0.060
d_{z^2}	0.001	0.002
d_{tot}	0.120	0.164

[a] The C_4 axis lies in z direction. Cf. Figure 1, bottom middle.

Stabilization by sd hybridization also is obvious for the D_{4h} structure **5** of Ba_2H_4 (cf. Table IX). The Ba metal charge is the same as that for Ca in **5** (M = Ca), due to compensation: the d_{xy} and d_{xz} populations are larger, the s and p populations are smaller. The stabilizing contributions from cation polarization and the destabilization by anion–anion repulsion are both expected to be largest for this rather anisotropic metal environment. Consequently, the relative energy of this arrangement is most competitive for the heavy Ba dication (cf. section **III**).

VI. Vibrational Frequencies

The alkaline-earth hydrides and their dimers may be accessible experimentally by matrix-isolation techniques. In particular, vibrational spectroscopy should be useful for the characterization of these species. To facilitate the identification and structural characterization of the alkaline-earth dihydride dimers, we have calculated the HF harmonic vibrational frequencies for several possible stationary points on the M_2H_4 potential energy surfaces.

The frequencies and symmetry assignments for structures corresponding to minima (i.e. those with no imaginary frequencies) are given in Tables X–XII. Unscaled HF stretching frequencies are overestimated typically by 5–10%. Table XIII compares calculated (at the same level used for M_2H_4) and experimental[33] frequencies for the *monohydrides* MH (M = Mg, Ca, Sr, Ba). For these cases, the agreement is in fact much better than 5%. Very soft bending modes may exhibit considerably larger errors, both in the calculations and in the matrix experiments (due to interactions between host and guest molecules).[12] Thus, e.g., optimization of Sr_2H_4 in the C_{2h} symmetry, employing the contracted metal basis set used for the frequency calculations, converged to the D_{2h} structure **1**. On the other hand, the

(33) Huber, K. P.; Herzberg, G. *Constants of Diatomic Molecules*; Van Nostrand-Reinhold: New York, 1979.

Table X. Harmonic Vibrational Frequencies (cm^{-1}) and Symmetry Assignments for M_2H_4 in D_{2h} **1** (M = Mg, Ca), C_{2h} **2** (M = Sr, Ba), and C_{2v} Symmetry **3** (M = Ba)

D_{2h}	Mg	Ca	act.[a]	C_{2h}	Sr	Ba	act.[a]	C_{2v} (3)	Ba
B_{2g}	349	137	Ra	B_u	83	94	IR	B_2	84
B_{3u}	258	139	IR	A_g	47	99	Ra	A_1	91
A_g	345	212	Ra	A_g	131	156	Ra	A_1	99
B_{2u}	396	233	IR	A_u	191	206	IR	A_2	205
B_{3g}	292	244	Ra	B_g	204	321	Ra	B_1	273
B_{3u}	770	532	IR	B_u	455	456	IR	A_1	425
B_{2u}	1051	877	IR	A_u	803	706	IR	B_1	715
B_{3g}	1126	989	Ra	A_g	902	802	Ra	A_1	797
A_g	1380	1028	Ra	B_g	910	882	Ra	A_2	863
B_{1u}	1280	1110	IR	B_u	1009	981	IR	B_2	964
B_{1u}	1637	1306	Ra	A_g	1188	1088	Ra	B_2	1091
A_g	1647	1316	IR	B_u	1196	1095	IR	A_1	1094

[a] Ra = Raman-active mode; IR = IR-active mode.

Table XI. Harmonic Vibrational Frequencies (cm^{-1}) and Symmetry Assignments for C_{3v} M_2H_4 **4**

M	Ca	Sr	Ba
A_1	263	164	113
E	252	212	213
E	614	585	510
E	703	662	645
A_1	891	833	768
E	1097	1001	912
A_1	1226	1126	1049
A_1	1274	1154	1050

Table XII. Harmonic Vibrational Frequencies (cm^{-1}) and Symmetry Assignments for D_{4h} M_2H_4 **5**

M	Ca	Sr	Ba	act.[a]
A_{1g}	331	208	144	Ra
B_{2u}	75	428	624	IR
E_g	540	560	625	Ra
E_u	768	705	633	IR
B_{2g}	974	905	794	Ra
E_u	979	897	845	IR
B_{1g}	831	787	847	Ra
A_{2u}	941	912	912	IR
A_{1g}	1147	1050	987	Ra

[a] Ra = Raman-active mode; IR = IR-active mode.

Table XIII. Comparison of Calculated (SCF) and Experimental Harmonic Vibrational Frequencies (cm^{-1}) for the Monohydrides MH (M = Mg, Ca, Sr, Ba)

	calcd[a]	exptl[b]		calcd[a]	exptl[b]
MgH	1510	1495	SrH	1200	1206
CaH	1301	1298	BaH	1141	1168

[a] Same basis-set level as used for the dihydride dimers. [b] Cf. ref 33.

uncontracted basis set yielded an H_t–M–M angle of ca. 160° (cf. section IV). Clearly, higher theoretical levels are needed to obtain accurate vibrational frequencies for these very soft deformation modes (as has been shown previously for various alkaline-earth dihalides[11,12]).

Doubly bridged (C_{2h} **2** or D_{2h} **1**) and triply bridged (C_{3v} **4**) structures might be differentiated simply on the basis of the number of observable modes. Due to a higher degree of degeneracy (E representations), the C_{3v} arrangement should exhibit fewer vibrational bands than the C_{2h} or D_{2h} arrangements (cf. Tables X and XI). However, the inversion symmetry of the latter structures warrants that the bands are observable either only in the IR spectrum or only in the Raman spectrum. Hence, the number of observable bands by IR or Raman spectroscopy may be fewer than for the C_{3v} structures.

In the M–H stretching vibration region (>700 cm^{-1} for the heavier metals), the D_{2h} and C_{2h} structures exhibit only three IR-allowed modes (Table X). For the C_{3v} arrangements, four modes may in principle be observed (Table XI). Unfortunately, two of them (A_1) are almost degenerate for M = Sr and Ba. However, the spacing of the bands is much larger for C_{2h} than for C_{3v}. In contrast to the doubly and triply bridged structures, no high-energy terminal M–H_t stretching vibrations should be observable for the D_{4h} structures (Table XII). Using the calculated values as a guide, vibrational spectroscopy should be able to discriminate between the possible M_2H_4 structures.

In a very recent study of species obtained in photochemical reactions between calcium atoms and H_2 in a Kr matrix, Xiao et al.[34] observed bands at 1124, 1024, 870, and 597 cm^{-1}. They assigned these tentatively to Ca_2H_4, with an assumed doubly bridged structure. The agreement with our calculated Ca–H stretching frequencies (ca. data for **1**, Table X) is variable; e.g. the calculations would overestimate the frequency of the 1124-cm^{-1} band by ca. 16% (B_{1u}), but underestimate the 597-cm^{-1} mode by ca. 11% (B_{3u}). In contrast, our calculated data for the CaH_2 monomer[3] exhibit the typical ca. 10% overestimate compared to the data of Xiao et al.[34] Thus, at present, the origin of the bands assigned to Ca_2H_4 is uncertain.

VII. Discussion

Sr_2H_4 and particularly Ba_2H_4 prefer triply bridged C_{3v} structures **4** rather than the planar doubly bridged D_{2h} arrangement **1** expected from simple electrostatic considerations or by analogy with Be_2H_4[23-26] and Mg_2H_4.[26] Ca_2H_4 is intermediate in behavior; the D_{2h} form is favored but only slightly. The planar D_{2h} geometries **1** are not even minima for Sr_2H_4 and Ba_2H_4, but are transition structures (two imaginary frequencies) interrelating C_{2h} **2** and C_{2v} **3** with pyramidal metal coordination. Even the quadruply bridged D_{4h} **5** with extremely unsymmetrical metal coordination becomes competitive for Ba_2H_4.

Our unusual structural predictions for the dihydride dimers receive striking experimental support from the X-ray analyses of the dinuclear barium alkoxide $Ba_2(OCPh_3)_4(THF)_3$ (**7**) and of the siloxide $Ba_2(OSi^tBu_3)_4(THF)$ (**8**).[16] Both structures exhibit three bridging and one terminal alkoxide (or siloxide) ligand, directly comparable to our C_{3v} forms **4** for Ba_2H_4 and Sr_2H_4 (cf. Figure 1d)! The barium atom Ba(2) without a terminal anionic ligand is further coordinated by two (in **7**) or by one (in **8**) THF (Ba(1) also bears an additional THF ligand in **7**). The Ba–O_b distances in **7** and **8** are somewhat less regular than the Ba–H_b distances in Ba_2H_4 (C_{3v} structure **4**, Table IV), presumably due to steric repulsions between the bulky ligands.

Thus, dinuclear Ba_2X_4 complexes may indeed prefer triply bridged over doubly bridged arrangements. Chisholm, Caulton, and co-workers attributed the unexpected structures of **7** and **8** to the need for a location of negative charge between the two metal dications or to a need for an increase in the metal coordination number.[16] However, the present results for the simple M_2H_4 molecules (cf. in particular section V) strongly suggest that the inherent preference for unsymmetrical metal

(34) Xiao, Z. L.; Hauge, R. H.; Margrave, J. L. *High. Temp. Sci.* **1992**, *31*, 59.

coordination[3,5-12] is responsible for the C_{3v} arrangement of the XMX_3M cores in **7** and **8**.

Chisholm, Caulton, et al. noted[16] that the only other examples of similar XMX_3M arrangements are found with $Sn^{II}X_3M'$ species. Calculations on the heavy group 14 dihydride and difluoride dimers M_2X_4 (M = Ge, Sn, Pb; X = H, F) by Trinquier et al.[28] show a large preference for pyramidal (cf. C_{2h} **2**) over planar (D_{2h} **1**) structures. Gas-phase electron diffraction studies on Ge_2F_4 indicate a similar preference.[35] However, the presence of a stereochemically active lone pair dictates the reduced symmetry of these group 14 metals in their +II oxidation state. Other factors are responsible for Sr_2X_4 and Ba_2X_4. Large cation size (which reduces anion–anion repulsions), large cation polarizability, and readily available acceptor d orbitals on the cation all favor a reduction of the local symmetry around the metal in heavy alkaline-earth and lanthanide(II) MX_2 compounds.[5-13] The absence of π bonding in the hydrides also contributes to rather large deviations from symmetrical metal coordination.[5,8] The tendencies of SrH_2 and BaH_2[3] (and of many more SrX_2 and BaX_2 compounds[5,6,11,12]) to bend find their extension in the unusual dihydride dimer and in the alkoxide structures **7** and **8**,[16] in the pyramidal metal coordination exhibited by the dinuclear diamides $\{M[N(SiMe_3)_2]_2\}_2$ (M = Sr, Ba),[14] in the pyramidal structures of cationic complexes $M^{+2}(L)_3$,[7] and in the cisoid arrangement of the anionic ligands in solvated complexes $BaX_2(L)_n$.[15]

The structures of larger clusters or even of bulk MH_2 or MX_2 also are influenced by the preference of the heavier alkaline-earth metals for unsymmetrical over symmetrical coordination (note that the coordination chemistry of the lanthanides in their +II states exhibits very similar tendencies[6,9,10]). The trinuclear barium siloxide complex $[Ba_3(OSiPh_3)_6(THF)]\cdot 0.5THF$ (**9**)[36] extends the building principle exhibited by the dinuclear complexes **7** and **8**.[16] Remarkably, **9** has one barium atom with no terminal ligand—only contacts to four bridging siloxides. This results in a local metal coordination similar to that in the D_{4h} structure **5** of Ba_2H_4 (cf. Figure 1, bottom middle). Even larger octanuclear aryloxide clusters with very asymmetric metal environments[37] are noteworthy in this context.[38]

In the solid state, the dihydrides MH_2 (M = Ca, Sr, Ba, Yb, Eu, Sm) also exhibit rather unsymmetrical metal coordination (by seven more closely and two more loosely bound ligands in a $PbCl_2$-type structure[1,39]). While crystal-field effects on d orbitals have been discussed for solid EuH_2,[39b] no covalent bonding or cation polarization arguments have been evoked for the CaH_2, SrH_2, or BaH_2 solid-state structures. These and related arrangements of extended systems with unsymmetrical metal coordination (e.g. various group 2 or lanthanide dihalide solid-state structures) might also be due to d-orbital participation in bonding and to cation polarization. Explicit calculations on the bulk systems or on larger clusters are desirable.

The molecular dihydrides of the heavy alkaline-earth metals and their dimers are not known experimentally. However, they might be accessible by molecular beam and matrix-isolation techniques (cf. ref 34). The calculated vibrational frequencies for the dihydrides[3] and for various structural alternatives of their dimers should aid in the experimental identification of these species.

Acknowledgment. This work was supported by the Deutsche Forschungsgemeinschaft, the Fonds der Chemischen Industrie, the Stiftung Volkswagenwerk, and Convex Computer Corporation. M.K. is grateful to Prof. Dr. H. G. von Schnering for providing computer facilities at the MPI. We thank Dr. M. Westerhausen (Stuttgart) for his interest and helpful suggestions.

(35) Huber, H.; Künding, E. P.; Ozin, G. A.; Van der Voet, A. *Can. J. Chem.* **1974**, *52*, 95.

(36) Caulton, K. G.; Chisholm, M. H.; Drake, S. R.; Streib, W. E. *Angew. Chem.* **1990**, *102*, 1492; *Angew. Chem., Int. Ed. Engl.* **1990**, *29*, 1483.

(37) Caulton, K. G.; Chisholm, M. H.; Drake, S. R.; Folting, K.; Huffman, J. C. *Inorg. Chem.* **1993**, *32*, 816.

(38) These alkoxide, aryloxide, and siloxide complexes are of interest as molecular precursors for the synthesis of superconducting ceramics containing Sr or Ba. Cf., e.g., refs 36 and 37.

(39) (a) Fischer, F.; Schefer, J.; Ticky, K.; Bischof, R.; Kaldis, E. *J. Less-Common Met.* **1983**, *94*, 151. (b) Bischof, R.; Kaldis, E.; Wachter, P. *J. Less-Common Met.* **1985**, *111*, 139. Holley, C. E.; Mulford, R. N. R.; Ellinger, F. H.; Koehler, W. C.; Zachariasen, W. H. *J. Phys. Chem.* **1955**, *59*, 1226.